UCSF
UC San Francisco Previously Published Works

Title

The Proprotein Convertase Subtilisin/Kexin Type 9 (PCSK9) Active Site and Cleavage Sequence Differentially Regulate Protein Secretion from Proteolysis*

Permalink

https://escholarship.org/uc/item/5460h2c9

Journal

Journal of Biological Chemistry, 289(42)

ISSN

0021-9258

Authors

Chorba, John S
Shokat, Kevan M

Publication Date

2014-10-01

DOI

10.1074/jbc.m114.594861

Peer reviewed

The Proprotein Convertase Subtilisin/Kexin Type 9 (PCSK9) Active Site and Cleavage Sequence Differentially Regulate Protein Secretion from Proteolysis*

John S. Chorba[‡§1] **and Kevan M. Shokat**[§¶]

From the ‡*Division of Cardiology, San Francisco General Hospital, Department of Medicine, University of California, San Francisco, California 94110,* §*Cardiovascular Research Institute, University of California, San Francisco, California 94158, and* ¶*Department of Cellular and Molecular Pharmacology, University of California, San Francisco, California 94158 and Department of Chemistry, University of California, Berkeley, California 94720*

Background: PCSK9 inhibition shows promise in the treatment of hypercholesterolemia and prevention of atherosclerotic heart disease.
Results: PCSK9 proteolysis and secretion have different structural requirements near the protein active site.
Conclusion: PCSK9 proteolysis and secretion occur in two separate steps.
Significance: The PCSK9 active site can serve as an allosteric modulator of protein secretion, suggesting a new strategy for inhibition.

Biologic-based strategies to inhibit proprotein convertase subtilisin/kexin type 9 (PCSK9) show promise as anti-hypercholesterolemic and, therefore, anti-atherosclerotic therapies. Despite substantial effort, no small molecule strategy to inhibit PCSK9 has demonstrated feasibility. In this study we interrogated the chemistry of the PCSK9 active site and its adjacent residues to identify a foothold with which to drug the PCSK9 processing pathway and ultimately disrupt the interaction with the LDL receptor. Here, we develop a system in which we amplify the readout of PCSK9 proteolysis with a highly specific substrate in cells, showing that the PCSK9 catalytic domain is capable of proteolysis in *trans*. We use this system to show that the substrate specificity for PCSK9 proteolysis is distinct from the specificity for PCSK9 secretion, demonstrating that PCSK9 processing occurs in two separate sequential steps: that of proteolysis followed by secretion. We show that specific residues in the protease recognition sequence can differentially modulate the effects on proteolysis and secretion. Additionally, we demonstrate that the clinically described, dominant negative Q152H mutation restricts proteolysis and secretion independently. Our results suggest that the PCSK9 active site and its adjacent residues serve as an allosteric modulator of protein secretion independent of its role in proteolysis, revealing a new strategy for intracellular PCSK9 inhibition.

Proprotein convertase subtilisin/kexin type 9 (PCSK9)[2] binds to the LDL receptor (LDL-R) on the hepatocyte cell surface, targeting it for lysosomal degradation (1, 2). By decreasing the available LDL-R, PCSK9 causes serum LDL cholesterol to increase, promoting atherosclerosis and heart disease (3). Due to a wealth of robust genetic data (4–7) and a well elucidated biochemical mechanism (8–11), PCSK9 has become a well validated target to treat hypercholesterolemia and, by extension, prevent atherosclerotic heart disease. Indeed, multiple strategies to inhibit the function of PCSK9 have reached clinical proof-of-principle (12–15). However, no small molecule approach is among them.

Although a small molecule strategy to inhibit PCSK9 is highly desirable, the cellular life cycle of PCSK9 offers insight into the challenge that small molecules face. Biochemically, PCSK9 is a protease, and the presence of an active site suggests it is a tractable drug target. However, among proteases it is unusual; its only known target is itself, and it undergoes only a single-turnover reaction. Proper self-cleavage, however, is critical for its function; after translocation to the endoplasmic reticulum (ER) and removal of the signal sequence, the proPCSK9 species undergoes intramolecular proteolysis. The cleaved, mature PCSK9 is trafficked through the *trans*-Golgi network and secreted into the extracellular space (Fig. 1*A*) where it reaches its target, the LDL-R (16–19). Because PCSK9 proteolysis is necessary for proper secretion (Fig. 1, *A* and *B*) (18, 20) and subsequently the extracellular interaction with the LDL-R, inhibiting proteolysis has been proposed as a therapeutic strategy. However, this approach has been remarkably difficult to achieve (15, 21). After self-proteolysis, the C terminus of the prodomain remains non-covalently bound to the active site

1 To whom correspondence should be addressed: Division of Cardiology, San Francisco General Hospital, Dept. of Medicine, University of California, San Francisco, 600 16th St., San Francisco, CA 94158-2280. Tel.: 415-502-1475; Fax: 415-514-0822; E-mail: john.chorba@ucsf.edu.

2 The abbreviations used are: PCSK9, proprotein convertase subtilisin/kexin type 9; LDL-R, LDL receptor; CHR, cysteine-histidine rich; ER, endoplasmic reticulum; Ni-NTA, nickel nitrilotriacetic acid; Bis-Tris, 2-[bis(2-hydroxyethyl)amino]-2-(hydroxymethyl)propane-1,3-diol; SS, signal sequence; Cat, catalytic.

and is thought to act as a self-inhibitor, preventing any further proteolytic activity (22). *In vitro* methods of measuring PCSK9 proteolytic activity struggle from the low intrinsic activity of the protease, requiring high amounts of purified protein and producing low signal-to-noise ratios (23). In addition, the prodomain cannot be removed from the catalytic domain short of denaturing the entire protein, and no group has isolated the proteolytically active proPCSK9 form (24). Last, even if an inhibitor for the PCSK9 protease was found, it would likely need to outcompete an intramolecular reaction to be clinically useful.

Chemical challenges are not atypical for protease inhibitors. Direct renin inhibitors serve as an example that these challenges can be overcome; after decades of focused effort, a structure and modeling approach produced aliskiren, now a clinically approved compound (25, 26). Our understanding of PCSK9 processing and maturation suggests that the difficulty in targeting PCSK9 proteolysis is primarily one of active site accessibility. We thus undertook the present study to thoroughly investigate the biochemistry of the PCSK9 active site. Our primary goal was to identify any unusual aspects that would allow us a foothold into a possible small molecule approach to perturb PCSK9 proteolysis or secretion.

EXPERIMENTAL PROCEDURES

Materials and Reagents—Oligonucleotide primers were custom synthesized by Elim Biopharmaceuticals (Hayward, CA). Restriction enzymes and polymerases were purchased from New England Biolabs (Ipswich, MA). Mouse monoclonal antibodies to FLAG (clone M2) and V5 (clone V5–10) and anti-FLAG M2 magnetic beads were obtained from Sigma. Mouse monoclonal antibody to penta-His and Ni-NTA-agarose were obtained from Qiagen (Valencia, CA). Mouse monoclonal antibody to β-actin (8H10D10), rabbit monoclonal antibody to GFP (D5.1 XP), which also detects cyan and yellow fluorescent protein, goat anti-rabbit IgG HRP-conjugate antibody, and horse anti-mouse IgG HRP-conjugate antibody were all obtained from Cell Signaling (Danvers, MA). Rabbit polyclonal antibody to transferrin was obtained from Enzo Life Sciences (Farmingdale, NY). Goat anti-mouse IgG IRDye 800CW conjugate and goat anti-rabbit IgG IR Dye 800CW conjugate were obtained from LI-COR Biotechnology (Lincoln, NE).

Plasmid Construction—PCSK9 expression vectors were created by PCR amplification of the appropriate PCSK9 domains from pCMV-PCSK9-FLAG (generously provided by Prof. J. Horton, UT Southwestern) with custom oligonucleotides and subsequent cloning into the BglII and NotI restriction sites of pIRES2-AcGFP1 and pIRES2-DsRed2 (Clontech, Mountain View, CA). V5, HA, and His$_6$ tags, VFAQSIP insertions, and single site mutations were added by site-directed mutagenesis using partially overlapping primers to generate the constructs as shown in the schematics (27). Truncations of the prodomain C terminus, prodomain, and removal of the vector sequence encoding the fluorescent proteins were also performed by site-directed mutagenesis using partially overlapping primers. Expression vectors encoding FRET substrates were created by Gibson assembly (28) after PCR amplification of CyPET and YPET from pB33-newCyPET-LVPRGS(Sub)-YPET (gener-

ously provided by Dr. T. Shropshire and Prof. P. Daugherty, UC Santa Barbara) and using the PCSK9 expression vectors as a backbone. All plasmids were extensively sequenced to confirm their identities.

Mammalian Cell Culture and Transfections—HEK293T cells (ATCC, Manassas, VA) were cultured in DMEM with 10% FBS. Cells were plated in 6-well plates coated with poly-L-lysine (Sigma) 1 day before transfection to obtain ~50–75% confluency at the time of the experiment. Cells were transfected with Lipofectamine 2000 (Invitrogen) according to the manufacturer's instructions using 0.5 μg of DNA per construct. The medium was changed 6–8 h after transfections; for samples in which the conditioned media was evaluated the medium was changed to DMEM with 1× insulin-transferrin-selenium (Invitrogen) rather than DMEM with 10% FBS. After 48–72 h post-transfections, the cells and conditioned media (if appropriate) were harvested for Western blot analyses. The conditioned media was centrifuged for 5 min at 1000 × g, and the resulting supernatant was concentrated ~10× using Amicon Ultra 10 kDa protein concentrators (EMD Millipore, Billerica, MA). The cells were washed twice with ice-cold PBS, lysed in lysis buffer (50 mM Tris-HCl, pH 7.4, 150 mM NaCl, 0.1% Nonidet P-40, 0.5% Triton X-100) for 10 min, and then clarified at 21,000 × g for 15 min. Protein concentration was analyzed by Bradford assay (Bio-Rad). Gel samples were prepared with a SDS-based loading buffer under reducing conditions and heated at 98 °C for 5 min. All transfection experiments were repeated at least three times to ensure reproducibility.

Ni-NTA Pulldown Assays—Conditioned media from transfections was adjusted to pH 8.0 with Tris-HCl to a final concentration of 50 mM, and imidazole was added to a final concentration of 10 mM. The medium was centrifuged at 1000 × g, and the supernatant was added to Ni-NTA-agarose beads (Qiagen) previously equilibrated in binding buffer (20 mM Tris-HCl, pH 8.0, 250 mM NaCl, and 10 mM imidazole). Medium was batch-bound for 4 h with rotation at 4 °C. The beads were washed 3 times with 10× volumes of wash buffer (20 mM Tris-HCl, pH 8.0, 250 mM NaCl, 20 mM imidazole). Elution was performed with 5× volumes of elution buffer (20 mM Tris-HCl, pH 8.0, 250 mM NaCl, 250 mM imidazole) with the supernatant saved and the process repeated. The fractions were pooled and concentrated ~10× in Amicon Ultra 10-kDa concentrators. The concentrated samples were then prepared for gel analysis using a SDS-based loading buffer under reducing conditions and heated at 98 °C for 5 min.

Anti-FLAG Immunoprecipitations—Transfected cells were lysed on ice for 10 min in lysis buffer containing a protease inhibitor mixture (Roche Applied Science) and clarified at 21,000 × g for 15 min. The resultant supernatant was saved and subjected to Bradford assay. Equivalent amounts of lysate (according to total protein) were added to anti-FLAG M2 magnetic beads (Sigma) previously equilibrated in lysis buffer and bound at 4 °C with rotation overnight. The beads were then washed 3 times with 10× volumes of lysis buffer and once with 10× volumes of TBS. Elution was performed by incubation with 10× volumes of 0.1 M glycine, pH 3.0, at room temperature with rotation for 5 min. The process was repeated, and the elution fractions were pooled and concentrated ~10× in Ami-

can Ultra 10-kDa concentrators. The concentrated samples were then prepared for gel analysis using a SDS-based loading buffer under reducing conditions and heated at 98 °C for 5 min.

Western Blot Analyses—Gel samples were loaded onto 4–12% Bis-Tris SDS NuPAGE precast gels (Invitrogen) for electrophoresis. The size-separated proteins were then transferred to nitrocellulose. The blots were blocked in 5% nonfat dry milk in Tris-buffered saline (20 mM Tris, pH 7.4, 150 mM NaCl) containing 0.1% Tween (TBS-T) for 1 h. The appropriate primary antibodies were hybridized to the blots overnight at 4 °C. The blots were washed 3 times for 10 min each with TBS-T, and the appropriate secondary antibodies were hybridized in 5% nonfat dry milk in TBS-T for 1 h at room temperature. The blots were again washed 3 times for 10 min each with TBS-T before either developing with chemiluminescent substrate and imaging with CL-Xposure film (Thermo Fisher Scientific, Rockford, IL) or directly imaging with the ODYSSEY infrared imaging system (LI-COR Biotechnology, Lincoln, NE). Quantification was performed with the LI-COR Image Studio or Image Studio Lite software.

RESULTS

The PCSK9 Catalytic Domain Can Perform Intermolecular Proteolysis—We first endeavored to develop a robust method to evaluate PCSK9 proteolysis. To maximize both utility and specificity in our system, we focused on proteolysis in the native, cellular environment with a highly specific substrate. Although conversion of wild-type proPCSK9 to mature PCSK9 occurs in an intramolecular fashion (Fig. 1*A*) (17), McNutt *et al.* (29) demonstrated that the prodomain and catalytic domain can be assembled in *trans* (*i.e.* as two separate polypeptides), which effectively bypasses the need for proteolysis and does not require intrinsic proteolytic activity (Fig. 1, *C* and *D*). Furthermore, a secretion-defective PCSK9 mutant can transfer its prodomain to a prodomain-deficient (and also secretion-defective) PCSK9, rescuing the secretion of the latter PCSK9 species (30). As such, we hypothesized that the in *trans* assembly of the catalytic domain and a specific substrate and subsequently intermolecular proteolysis could also occur.

To evaluate this hypothesis, we designed a series of constructs to evaluate for the specific cleavage of a "substrate," a full-length but proteolytically inactive S386A mutant PCSK9 termed substrate$_{PCSK9}$, by a "protease," an orthogonally tagged PCSK9 construct containing the catalytic domain (Fig. 2*A*). Given that the S386A mutant is devoid of proteolytic activity, any cleavage of the substrate in our system must, therefore, come from an intermolecular cleavage event. Similarly, we used the S386A mutant in each protease construct throughout our investigation as a negative control. Co-transfection of a full-length PCSK9 protease, termed protease$_{PCSK9}$, with substrate$_{PCSK9}$ into HEK 293T cells revealed a trace amount of cleaved substrate$_{PCSK9}$ in the lysate (Fig. 2*B, lane 4, open arrows*). By contrast, co-transfection of the inactive protease$_{PCSK9-S386A}$ with substrate$_{PCSK9}$ produced no cleavage product (Fig. 2*B, lane 5*). Consistent with prior studies concluding that the vast majority of PCSK9 proteolysis is intramolecular (16, 17), the scale of intermolecular cleavage seen with protease$_{PCSK9}$ was far below (only ~1%) that of intramolecular
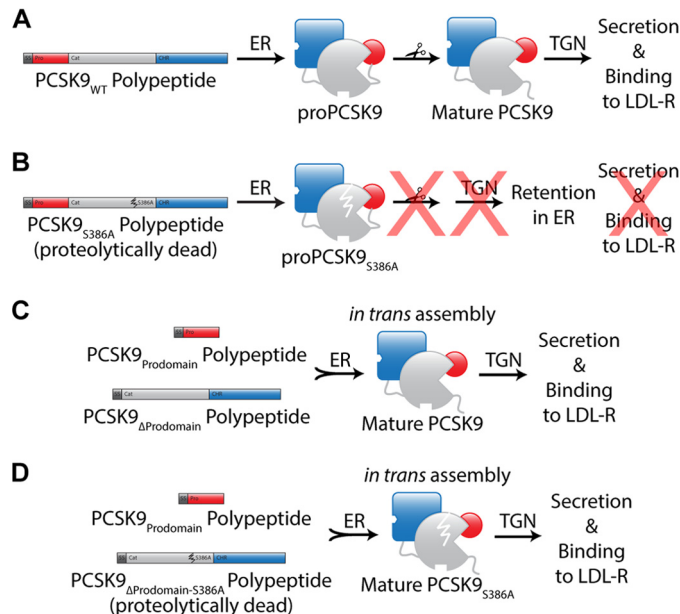

FIGURE 1. **Schematics of PCSK9 processing.** The known processing pathways of PCSK9 are shown. The signal sequence is shown in *dark gray*, the prodomain in *red*, the catalytic domain in *light gray*, and the CHR domain in *blue*. *A*, processing of wild-type PCSK9. The nascent PCSK9 polypeptide is directed to the ER by a signal sequence, which is subsequently removed by a signal peptidase. The proPCSK9 form then undergoes auto-proteolysis, and the mature, cleaved form is transported to the *trans*-Golgi network (*TGN*) via a COPII complex involving Sec24a. Secretion from the *trans*-Golgi network is facilitated by sortilin. The PCSK9 binds the LDL-R on the cell surface, chaperoning the receptor for lysosomal degradation upon internalization. *B*, processing of proteolytically inactive PCSK9. PCSK9 with an active site mutation (S386A) cannot perform intramolecular proteolysis, is retained in the ER, and thus cannot interact with the LDL-R on the cell surface. *C*, processing of in *trans* PCSK9. In an experimental system the prodomain and prodomain-deficient catalytic and CHR domains are expressed as separate polypeptides, each directed independently to the ER. These domains assemble in *trans*, bypassing the proteolytic step to form a mature PCSK9 that follows the remainder of the prototypic processing pathway and retains activity against the LDL-R. *D*, processing of in *trans* proteolytically inactive PCSK9. Because the proteolytic step is bypassed, a proteolytically inactive PCSK9 can be assembled in *trans* and secreted, retaining activity against the LDL-R.

cleavage of wild-type PCSK9 (Fig. 2, *B, lane 2* compared with *lane 4*, and *D, left, blue*). However, the co-transfection of a prodomain-deficient protease, termed protease$_{PCSK9\Delta Pro}$, markedly increased cleavage of substrate$_{PCSK9}$ (Fig. 2*B, lane 6*) when compared with protease$_{PCSK9}$ (Fig. 2*B, lane 4*) to just >15% of our wild-type benchmark (Fig. 2*D, right, blue*). In addition, the absence of cleaved substrate$_{PCSK9}$ with the co-transfection of inactive protease$_{PCSK9\Delta Pro-S386A}$ (Fig. 2*B, lane 7*) shows that the proteolysis of substrate$_{PCSK9}$ is highly specific for the active protease$_{PCSK9\Delta Pro}$. Furthermore, because protease$_{PCSK9\Delta Pro}$ is significantly more active than protease$_{PCSK9}$, these data show that the prodomain is a cis-acting inhibitor of intermolecular proteolysis, consistent with the known PCSK9 structure (22, 24, 31). We were particularly encouraged by our ability to amplify the detection of intermolecular PCSK9 proteolysis, especially given that the PCSK9 protease is thought to only undergo a single turnover event.

We then sought to evaluate whether the processed intermolecular cleavage products were properly secreted like wild-type PCSK9. To do so we evaluated the conditioned media of our co-transfections by Western blot (Fig. 2*C, left*). Secretion of protease$_{PCSK9\Delta Pro}$ occurred only in the presence of sub-
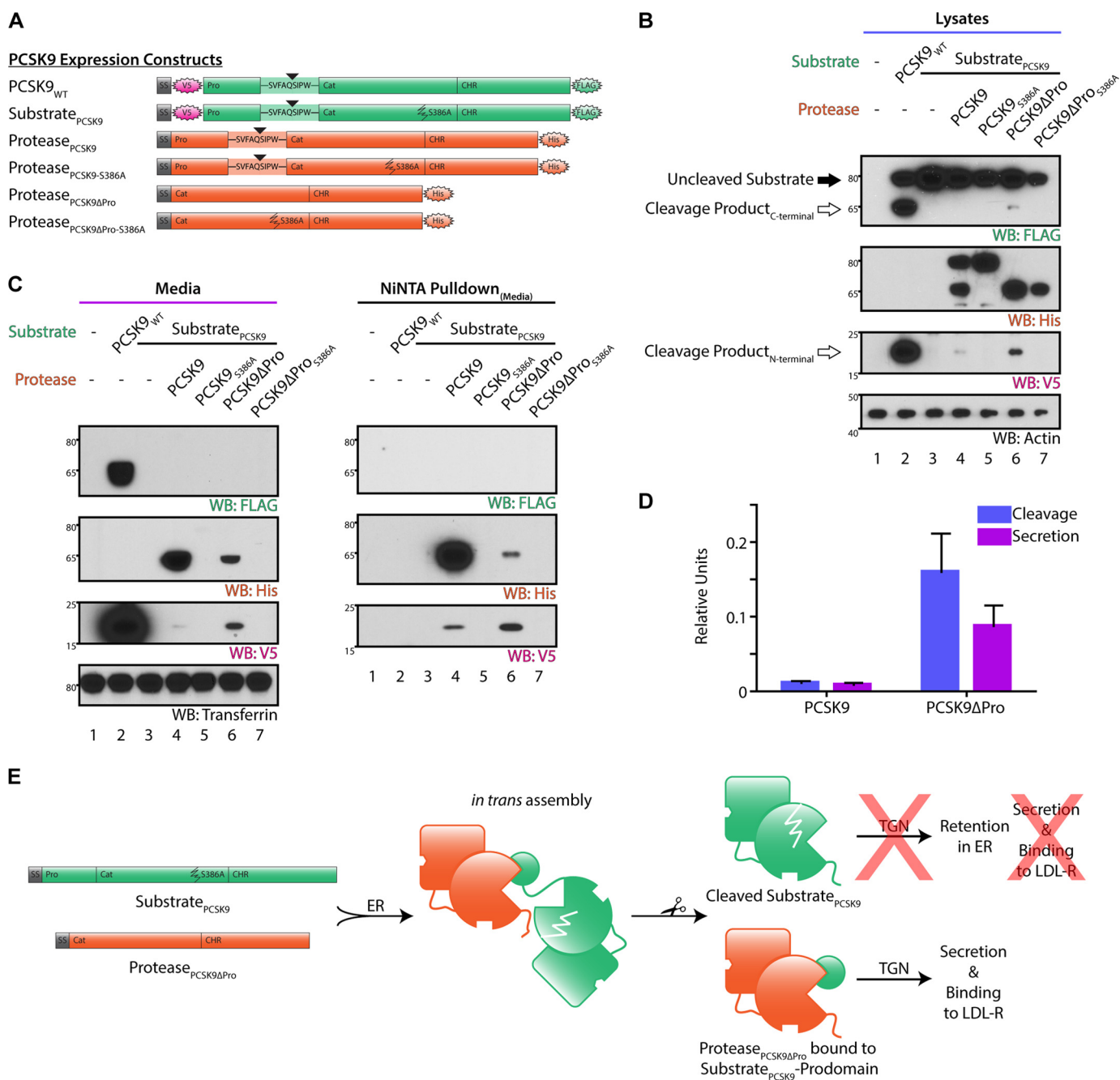
FIGURE 2. **The PCSK9 catalytic domain can perform proteolysis in *trans*.** *A*, schematics of the PCSK9 expression constructs. All PCSK9 expression constructs contain the N-terminal signal sequence and the appropriate PCSK9 domains as labeled. Domains within constructs are colored to correspond to the C-terminal recognition tag, orthogonal between protease and substrate constructs: *magenta*, V5 (N-terminal, substrate); *green*, FLAG (C-terminal, substrate); *orange*, His (C-terminal, protease). The P5 through P4′ sequence spanning the transition from the prodomain to catalytic domain is shown in wild-type PCSK9, substrate$_{PCSK9}$, and protease$_{PCSK9}$, with the cleavage site indicated by the *arrowhead*. The S386A mutation in substrate$_{PCSK9}$ is shown. *B*, Western blots (*WB*) of cell lysates from co-transfections of constructs or empty vectors into 293T cells as indicated. Wild-type PCSK9 (*lane 2*) serves as the positive control. Uncleaved substrate is noted by the *black arrow*. Cleavage products of substrate$_{PCSK9}$ are noted by the *open arrows*. *C*, Western blots of conditioned media (*left*) and Ni-NTA pulldown assays (*right*) from the same experiment as in *B*. *D*, mean levels of processed substrate$_{PCSK9}$ from either proteolysis (*blue*) or secretion (*purple*), as normalized to intramolecular proteolysis or secretion of wild-type PCSK9, respectively, from three independent experiments. *Error bars* represent S.E. *E*, model for processing of intermolecularly cleaved PCSK9. Protease$_{PCSK9ΔPro}$ recognizes the prodomain of substrate$_{PCSK9}$ in the ER in a manner akin to in *trans* assembly, performs intermolecular proteolysis, and then retains the "donor" prodomain from substrate$_{PCSK9}$. Protease$_{PCSK9ΔPro}$, with its donor prodomain, is capable of secretion following the prototypic PCSK9 secretion pathway, whereas the C-terminal cleavage product of substrate$_{PCSK9}$, without its prodomain, is retained in the ER. *TGN*, *trans*-Golgi network.

strate$_{PCSK9}$ and was accompanied by the prodomain from substrate$_{PCSK9}$ (Fig. 2*C*, *left*, *lane 6*) to levels of ∼10% that of wild-type PCSK9 (Fig. 2*D*, *right*, *purple*). By contrast, the inactive protease$_{PCSK9ΔPro-S386A}$ was not secreted in the presence of substrate$_{PCSK9}$ (Fig. 2*C*, *left*, *lane 7*). A trace amount (<1% of

wild type) of prodomain from substrate$_{PCSK9}$ was also secreted with protease$_{PCSK9}$ (Fig. 2*C*, *left*, *lane 4*, and Fig. 2*D*, *left*, *purple*). The C-terminal cleavage product of substrate$_{PCSK9}$, which contains the catalytic and cysteine-histidine-rich (CHR) domains, was not secreted under any condition (Fig. 2*C*, *left*).

Role of the PCSK9 Active Site in Proteolysis and Secretion

To confirm the association of the V5-tagged prodomain with the His-tagged protease$_{PCSK9\Delta Pro}$, we performed a pulldown experiment with Ni-NTA-agarose beads on the conditioned media to isolate the His-tagged protease$_{PCSK9}$ and protease$_{PCSK9\Delta Pro}$. This showed that the prodomain from substrate$_{PCSK9}$ co-precipitated with both proteases (Fig. 2C, right, lanes 4 and 6). Furthermore, there was proportionally much greater V5-tagged prodomain with protease$_{PCSK9\Delta Pro}$ than with protease$_{PCSK9}$ (Fig. 2C, right, compare lane 6 to lane 4). This likely results from a preference of protease$_{PCSK9}$ to utilize its own prodomain for secretion, which protease$_{PCSK9\Delta Pro}$ lacks. Overall, these data suggest that the prodomain is retained by the protease$_{PCSK9\Delta Pro}$ after intermolecular cleavage and are consistent with a model whereby the protease$_{PCSK9\Delta Pro}$ assembles with the prodomain of substrate$_{PCSK9}$, performs intermolecular cleavage, and then non-covalently retains the prodomain in a manner akin to intramolecularly processed PCSK9 (Fig. 2E). The prodomain from substrate$_{PCSK9}$ then serves as the chaperone guiding the mature protease$_{PCSK9\Delta Pro}$ out of the ER through the Golgi and ultimately to the extracellular space. Despite undergoing cleavage, the catalytic and CHR domains of substrate$_{PCSK9}$ have been stripped of their own prodomain and thus are not secreted.

The Scope of Intermolecular PCSK9 Proteolysis Is Narrow— Having identified an optimized, highly specific substrate for protease$_{PCSK9\Delta Pro}$, we next addressed the scope of the intermolecular cleavage reaction, as knowledge of the substrate specificity is an important first step toward inhibitor design. We asked whether the known cleavage sequence could be recognized and cut if placed elsewhere within the prodomain, anticipating that such engineering might generate a more active protease. We posed this hypothesis based on the typical processing pathway of proprotein convertases; most members of this family of proteases undergo two cleavage events to mature (32). The first event, common to all convertases including PCSK9, cuts the prodomain from the catalytic domain, allowing the prodomain to serve both as a chaperone for delivery of the convertase to its proper cellular compartment and a self-inhibitor of proteolytic activity (33). The second event, which PCSK9 does not perform, cleaves the prodomain at the flexible L loop, causing the prodomain to dissociate from the active site, releasing the self-inhibition on the proteolytic activity of the convertase (34). We, therefore, interrogated the small L loop of PCSK9, located after Lys-125, as well as an additional solvent-exposed loop of the prodomain at Pro-138 to evaluate whether an additional proteolytic event could occur. We inserted the seven-amino acid PCSK9 cleavage sequence VFAQSIP into our initial substrate construct between Lys-125 and Met-126 to create substrate$_{PCSK9-K125iSELF}$ and in place of Pro-138 and His-139 to create substrate$_{PCSK9-P138iSELF}$ (Fig. 3A). Co-transfection of substrate$_{PCSK9-K125iSELF}$ with protease$_{PCSK9\Delta Pro}$ revealed only a trace amount of cleaved product (Fig. 3B, left, open arrows, lane 3) with cleavage clearly less efficient than with unmodified substrate$_{PCSK9}$ (Fig. 3B, left, lane 2). Because of the low signal for cleavage of substrate$_{PCSK9-K125iSELF}$ in the lysates, we confirmed the presence of the N-terminal cleavage product in the conditioned media (Fig. 3B, right, open arrow, lane 3), indicating that it also permit-

ted secretion of the protease. Importantly, this cleavage product migrated at ~18 kDa and just above the prodomain of the unmodified substrate$_{PCSK9}$, consistent with a cleavage site at the native Gln-152 (anticipated molecular mass of ~17 kDa) rather than within the engineered sequence (anticipated molecular mass of ~13 kDa) (Fig. 3B, compare lanes 2 and 3). We did not detect a band at a lower molecular weight corresponding to the smaller cleavage product, indicating that cleavage within the engineered insertion sequence did not occur. By contrast, neither appreciable cleavage nor secretion of the protease occurred for substrate$_{PCSK9-P138iSELF}$ (Fig. 3B, lane 5) or for any conditions with inactive protease$_{PCSK9\Delta Pro-S386A}$ (Fig. 3B, lanes 4 and 6), indicating that the insertion in place of Pro-138/His-139 also prevented proteolysis of the native sequence. Because our insertions were purposefully non-conservative, we acknowledge that such mutagenesis may have disrupted the proper folding of the substrate$_{PCSK9}$, preventing it from forming a cleavable complex with protease$_{PCSK9\Delta Pro}$. However, because the complex of protease$_{PCSK9\Delta Pro}$ and the prodomain from substrate$_{PCSK9-K125iSELF}$ permits secretion, we know this is unlikely for this particular insertion. Although we cannot rule out the possibility that a VFAQSIP site placed elsewhere within the prodomain would be cleaved, our data show that the catalytic domain cannot identify and cleave its known recognition site when that site is placed within the prodomain L loop.

To further address the scope of this reaction, we next asked whether the PCSK9 catalytic domain could identify and cleave a minimal recognition sequence outside of the full PCSK9 protein. We generated minimal substrates consisting of the anticipated PCSK9 cleavage sequences VFAQSIPW and SSVFAQSIPWNL flanked by a fluorescent protein pair (CyPET-YPET) (35). Co-expression of either substrate with protease$_{PCSK9\Delta Pro}$ revealed no appreciable cleavage product (data not shown), suggesting that the catalytic domain requires at least another region of substrate$_{PCSK9}$ beyond the cleavage site itself to properly recognize and cleave its known sequence. When taken together with the results of Fig. 3, these data support the concept that the PCSK9 catalytic domain has a narrow specificity window for its known substrate.

The Prodomain Inhibits Intermolecular Proteolysis in trans, Dependent on Its C-terminal Tail—Having established both the capability and the relatively narrow scope of the PCSK9 catalytic domain for intermolecular cleavage, we next sought to identify a positive control for an inhibitor of the intermolecular proteolysis reaction. Based on the occupancy of the active site by the prodomain C terminus (22, 24, 31) as well as our own results of the prodomain inhibiting intermolecular proteolysis in *cis*, we hypothesized that exogenous prodomain would serve as a model inhibitor and effectively block intermolecular proteolysis in *trans*. To test this we performed co-transfections in the intermolecular cleavage system (protease$_{PCSK9\Delta Pro}$ acting upon substrate$_{PCSK9}$) with an additional wild-type prodomain construct termed prodomain$_{WT}$ (Fig. 4A). Co-transfection of protease$_{PCSK9\Delta Pro}$ with substrate$_{PCSK9}$ and prodomain$_{WT}$ revealed progressively less cleaved substrate with increasing
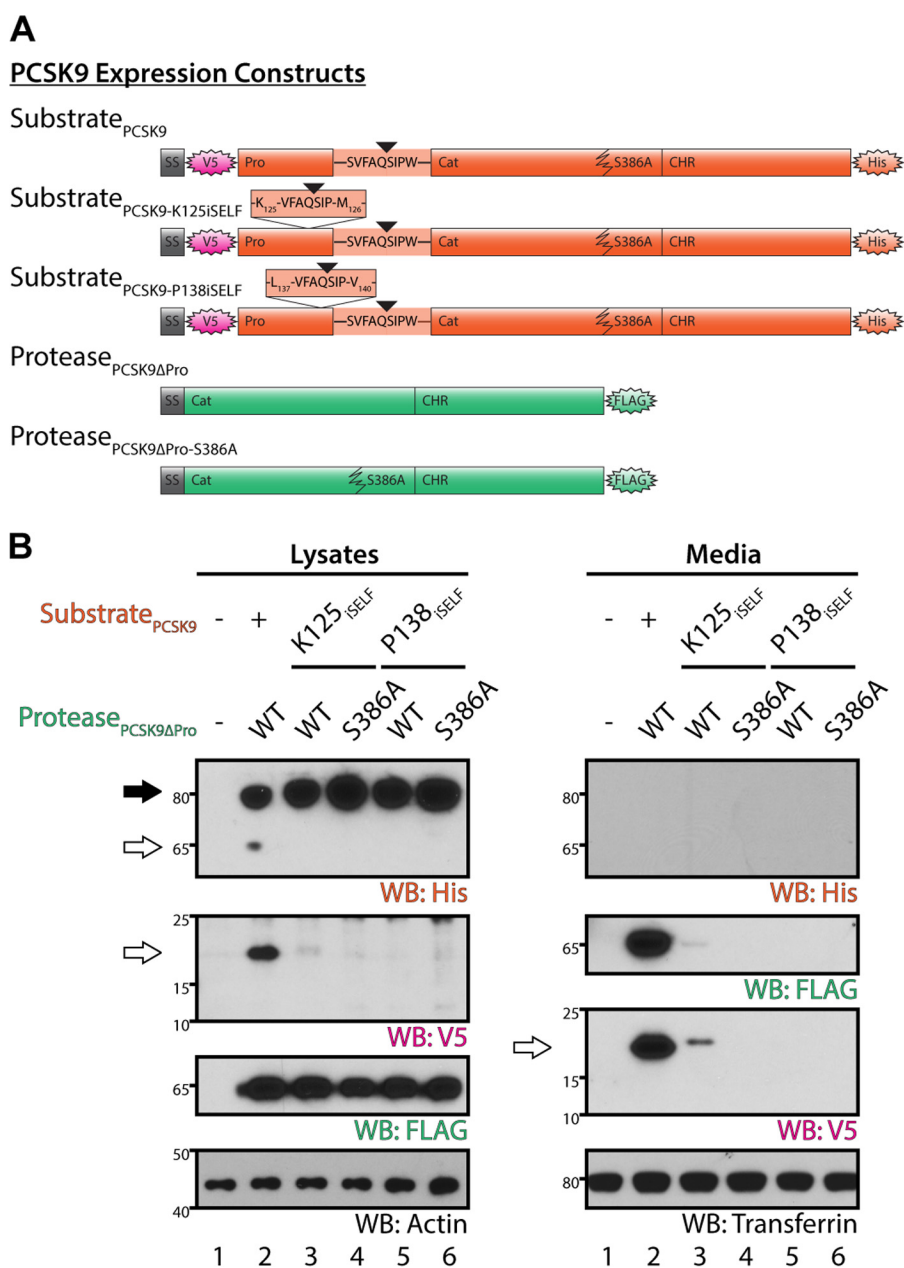
FIGURE 3. **The catalytic domain cannot cleave an engineered substrate sequence placed in the prodomain L loop.** *A*, schematics of the PCSK9 expression constructs. Domains tracking with the C-terminal tags are shown in the corresponding color: *magenta*, V5 (N-terminal, substrate); *orange*, His (C-terminal, substrate); *green*, FLAG (C-terminal, protease). A VFAQSIP substrate sequence is inserted between Lys-125 and Met-126 for substrate$_{PCSK9-K125iSELF}$ and in place of Pro-138 and His-139 for substrate$_{PCSK9-P138iSELF}$. The native VFAQSIP PCSK9 cleavage sequence in both substrates remains intact as shown. The expected cleavage sites are noted by the *arrowheads*. B, Western blots (*WB*) of cell lysates (*left*) and conditioned media (*right*) of co-transfections with the indicated constructs. Uncleaved substrate is noted by the *black arrow*. Substrate cleavage products are noted by the *open arrows*. The unmodified substrate$_{PCSK9}$ with protease$_{PCSK9\Delta Pro}$ (*lane 2*) serves as the positive control. Note that the V5-tagged N-terminal cleavage product of substrate$_{PCSK9-K125iSELF}$ migrates at a slightly greater molecular weight than that of substrate$_{PCSK9}$, indicating that the cleavage site is at the native Gln-152 rather than the engineered VFAQSIP sequence between Lys-125 and Met-126.

expression levels of the prodomain$_{WT}$ (Fig. 4*B*, *lanes 4–7*, and the graph below).

We next wished to carry out a structure-activity relationship study of the determinants of inhibition by the C-terminal tail of the prodomain. We created a series of mutant prodomain constructs harboring progressive amino acid deletions from the C terminus. We extended our truncations through the six amino acids spanning the entire binding groove of the active site, from the terminal Gln-152 to Ser-147, to create constructs prodomain$_{\Delta 152}$ through

prodomain$_{\Delta 147}$ (Fig. 4*A*). As anticipated, we found that at equivalent expression levels, the wild-type prodomain was the most effective inhibitor of intermolecular proteolysis (Fig. 4*C*, *lane 4*). Furthermore, the loss of even one amino acid from the C terminus markedly abrogated the inhibitory ability of the exogenous prodomain, as evidenced by the presence of more cleavage product (Fig. 4*C*, compare *lane 5* to *lane 4*, and the graph below). Importantly, further truncations did not result in progressively less effective inhibitors (Fig. 4*C*, *lanes 6-10*, and the graph below).

The Prodomain C Terminus Regulates Protein Secretion but Is Not Required for Catalytic Domain Binding—One potential explanation for these results is that the entire prodomain is required to bind to the catalytic domain and inhibit the intermolecular cleavage reaction. To evaluate this, we co-transfected our truncated prodomain$_\Delta$ constructs with protease$_{PCSK9\Delta Pro}$ to evaluate for the proper association of these domains in cells. Anti-FLAG immunoprecipitations of
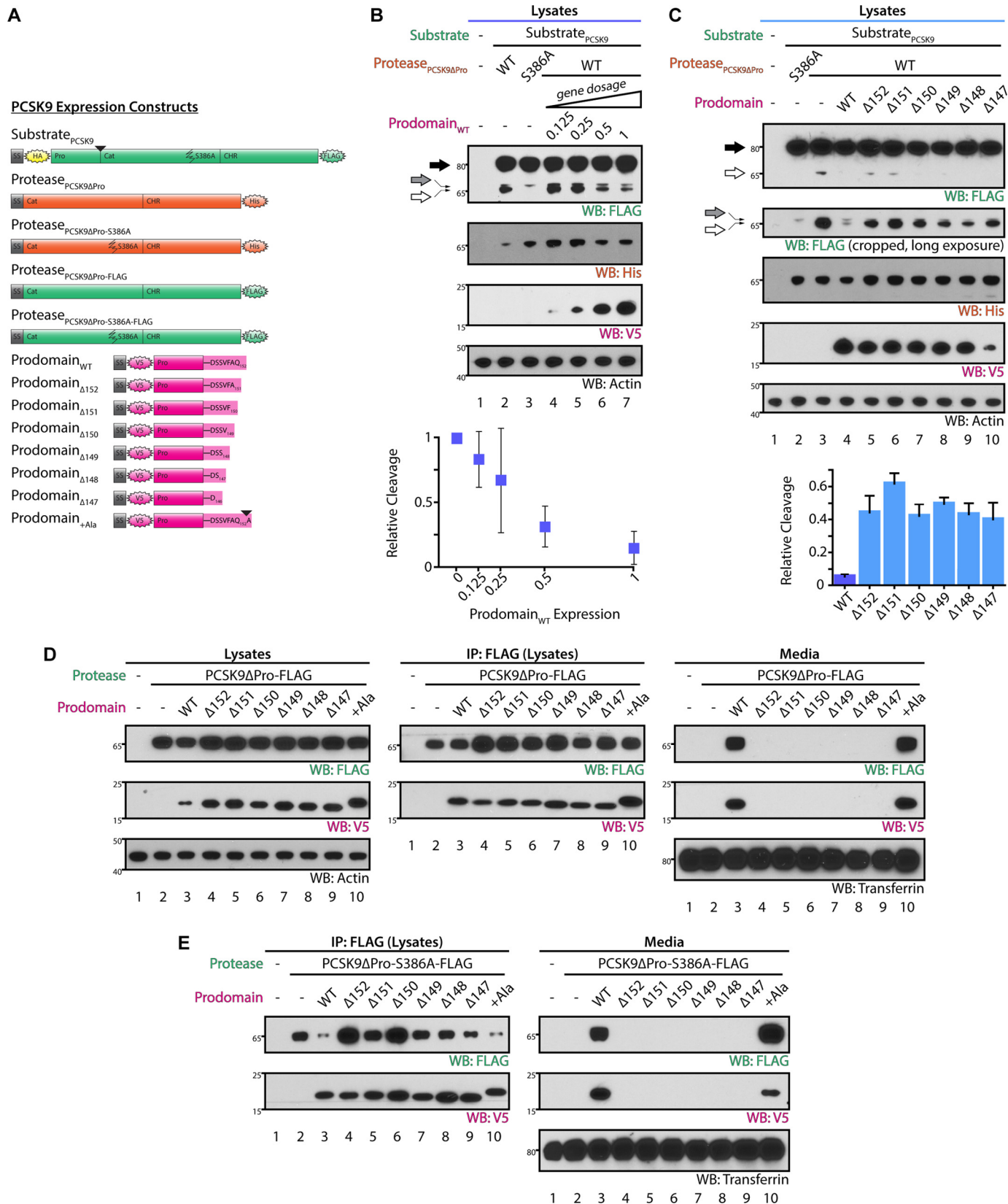
the lysates revealed that in all cases the V5-tagged truncated prodomains co-immunoprecipitated with the FLAG-tagged protease$_{PCSK9\Delta Pro}$ (Fig. 4D, *middle, lanes 3–9*). These results indicate that the truncated prodomains retain the ability to bind to the catalytic domain, although whether these complexes represent properly folded, mature PCSK9 or an aggregate of misfolded protein is less clear. Remarkably, however, when analyzing the media from these co-transfections, we found no secreted protease$_{PCSK9\Delta Pro}$-prodomain complexes, save for prodomain$_{WT}$ (Fig. 4D, *right, lanes 3–9*). To further probe the requirement of the C terminus in permitting secretion, we engineered a prodomain construct with an additional alanine inserted after Gln-152, termed prodomain$_{+Ala}$. Co-transfection of this construct with protease$_{PCSK9\Delta Pro}$ resulted in both intact prodomain:catalytic domain binding (Fig. 4D, *middle, lane 10*) as well as preserved secretion (Fig. 4D, *right, lane 10*). Importantly, all of these results held true for both the active protease$_{PCSK9\Delta Pro}$ and the inactive protease$_{PCSK9\Delta Pro-S386A}$ (Fig. 4E).

The Residues of the Prodomain C Terminus Regulate Proteolysis and Secretion Independently—We were struck by the exquisite sequence requirements of the prodomain$_\Delta$ constructs for secretion. To further evaluate these requirements, we performed an alanine scan of the prodomain C-terminal tail to investigate the effect of mutation of each residue on secretion. We created a series of prodomain constructs with alanine mutations from Ser-148 through Gln-152 along with the corresponding double, triple, and quadruple mutants. We then co-transfected protease$_{PCSK9\Delta Pro}$ with the prodomain mutants and analyzed the conditioned media (Fig. 5). We found that secretion was only mildly affected by alanine substitutions at Ser-148, Phe-150, and Gln-152 (Fig. 5B, *lanes 5, 7,* and *8* and Fig. 5C). By contrast, secretion was markedly abrogated by an alanine substitution at Val-149 (Fig. 5B, *lane 6,* and Fig. 5C). Similarly, secretion was abrogated for all double, triple, and quadruple mutants with the exception of the double mutants containing S148A, with the S148A/V149A mutant the most significantly affected among that subset (Fig. 5, *B, lanes 9–19,* and *C*). When the results from Figs. 4 and 5 are taken together, the findings suggest that the C terminus of the prodomain is critical for its proper function as a chaperone for PCSK9 secretion, with a strict requirement that all amino acids be present and a more lax requirement for the identity of the individual residues. The strict requirement for Val-149 is not surprising given that the isopropyl side chain points directly into the binding groove of the catalytic domain in the PCSK9 structure.
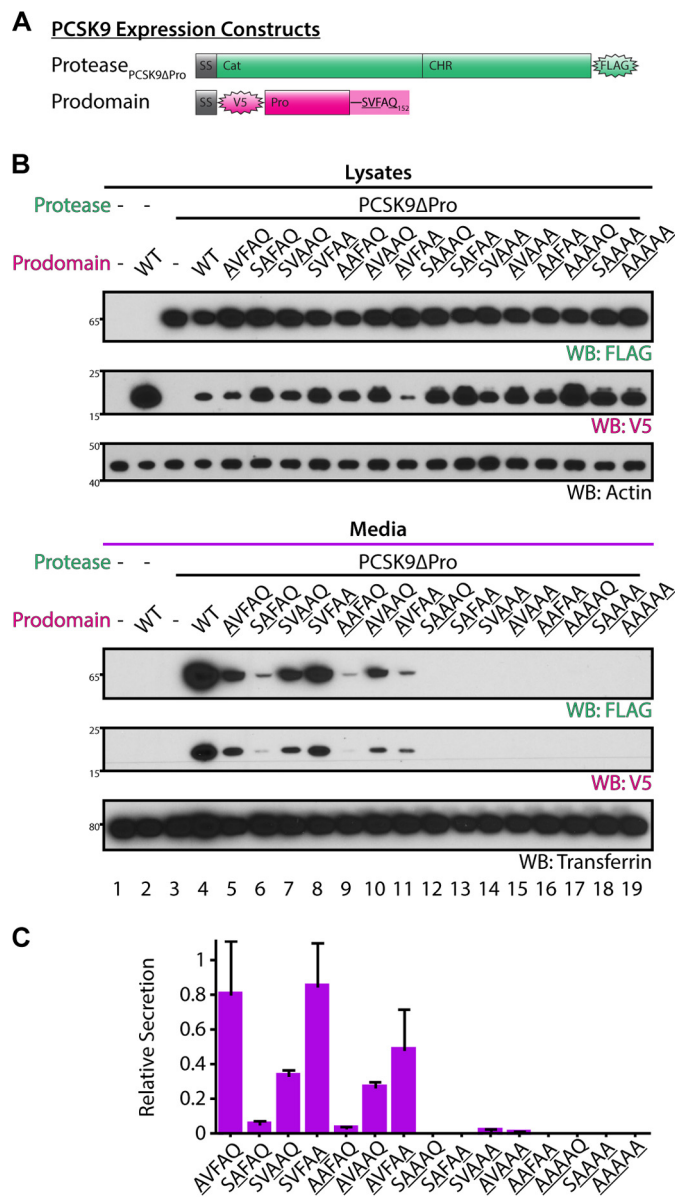

FIGURE 5. **An alanine scan of the prodomain C terminus reveals that Val-149 is critical for secretion.** *A*, schematics of expression constructs are shown. The prodomain C-terminal residues targeted for alanine mutation are *underlined*. *B*, Western blots (*WB*) of cell lysates (*top*) and conditioned media (*bottom*) of co-transfections of protease$_{PCSK9\Delta Pro}$ with mutant prodomains. Co-transfection of protease$_{PCSK9\Delta Pro}$ with wild-type prodomain serves as the positive control (*lane 4*). *C*, relative secretion of the protease$_{PCSK9\Delta Pro}$-prodomain complex for each alanine scan mutant, normalized to wild-type in *trans* PCSK9. Data are from two orthogonal readouts from two independent experiments, and *error bars* represent S.E.

FIGURE 4. **The prodomain inhibits intermolecular proteolysis *in trans* and requires the C terminus for full inhibition and proper secretion.** *A*, schematics of the expression constructs are again shown. Note that protease constructs with His tags (*orange*) correspond to *panels B* and *C*, and protease constructs with FLAG tags (*green*) correspond to *panels D* and *E*. The C-terminal residues of the prodomain constructs are shown. *B*, Western blots (*WB*) of cell lysates of co-transfections with exogenous prodomain. The gene dosage of prodomain construct relative to the protease construct is noted. Co-transfection of substrate and protease in the absence of exogenous prodomain serves as the positive control (*lane 2*). Uncleaved substrate is noted by the *black arrow*. Products of specific cleavage by protease$_{PCSK9\Delta Pro}$ are noted by the *open arrow*. A nonspecific cleavage product of substrate$_{PCSK9}$ is noted by the *gray arrow*. The *graph below* shows the relative cleavage of substrate$_{PCSK9}$ at increasing levels of exogenous prodomain, normalized to the absence of prodomain, from three independent experiments. *Error bars* represent S.E. *C*, Western blots of cell lysates of co-transfections with truncated prodomains. Co-transfection of substrate and protease in the absence of exogenous prodomain serves as the positive control (*lane 3*). The *graph below* shows the relative cleavage of substrate$_{PCSK9}$ in the presence of the prodomain mutants, normalized to the absence of exogenous prodomain. *Error bars* represent S.E. *D*, Western blots of cell lysates (*left*), FLAG-immunoprecipitations (*IP, middle*), and conditioned media (*right*) of co-transfections of protease with truncated prodomains. *E*, Western blots of FLAG-immunoprecipitations (*left*) and conditioned media (*right*) from the same experiment as in *D* but with proteolytically inactive protease.

However, the tolerability at Phe-150 is somewhat surprising given that the phenyl ring of this side chain makes a π-π stacking interaction with the indole of Trp-72 and is important for proper intramolecular cleavage of PCSK9 (16, 22).

We were intrigued by the differential structural requirements of the proteolytic site *vis à vis* the requirements for secretion in *trans* in a system that effectively bypasses the need for proteolysis. We next performed a serial alanine scan of the P5 through P4′ residues of substrate$_{PCSK9}$ to determine the tolerance for these mutations in our intermolecular cleavage system. Co-transfections of protease$_{PCSK9\Delta Pro}$ with the substrate$_{PCSK9}$ alanine scan mutants revealed that alanine substitutions at most positions were well tolerated, with the exception of P4 (Val-149) and P3 (Phe-150), where no cleavage occurred (Fig. 6, *B* and *C*). The intolerance for intermolecular cleavage for V149A was not surprising given prior work showing that this mutation abolishes intramolecular proteolysis (16) as well as our own results indicating that this mutation did not permit secretion. However, the lack of intermolecular cleavage of our F150A mutant was unexpected, as this mutant is known to permit a low level of intramolecular proteolysis (16). In addition, our results showed that the F150A modestly permitted secretion in the in *trans* system, highlighting the disconnect between secretion and intermolecular proteolysis. Overall, our data show that the F150A mutant is incapable of intermolecular proteolysis, but if such proteolysis is bypassed then the F150A mutant is capable of secretion. This also suggests that, at least for our intermolecular system, the process of secretion of mature PCSK9 from the ER does not occur in a one-step concerted mechanism with proteolysis but instead involves two separate events mediated by different complexes (*i.e.* proteolysis, followed by secretion).

Having identified differential prodomain requirements for secretion and intermolecular proteolysis, we desired to return to a physiologic system that would mimic a natural PCSK9 variant and look for a similar disconnect between secretion and intramolecular proteolysis. We thus focused on Gln-152 given that the Q152H mutation has been documented in a patient cohort as a dominant-negative, loss-of-function phenotype resulting in low serum LDL cholesterol and a reduced incidence of atherosclerotic heart disease (36, 37). We began with a vertical mutagenesis strategy at Gln-152 to evaluate the requirements on secretion, as others have demonstrated the requirement of Gln-152 on intramolecular proteolysis previously (37). We generated a series of Q152X mutations in our prodomain constructs and performed co-transfections of prodomain$_{Q152X}$ with protease$_{PCSK9\Delta Pro}$. Comparing the mutations that permitted secretion in our strategy (Fig. 7) to prior reports of mutations permitting proteolysis (37), we identified four phenotypes of residues according to the independent effects on proteolysis and secretion. We then installed representative mutations in both full-length PCSK9 and our substrate$_{PCSK9}$ constructs to confirm the effects of these mutations on intra- and intermolecular proteolysis and test alongside secretion. Fig. 8B shows the results of intramolecular proteolysis of the full-length PCSK9$_{Q152X}$ (*left*) and intermolecular proteolysis from protease$_{PCSK9\Delta Pro}$ on substrate$_{PCSK9-Q152X}$ (*right*), whereas Fig. 8C shows the results of secretion from the in *trans* assembly of

A

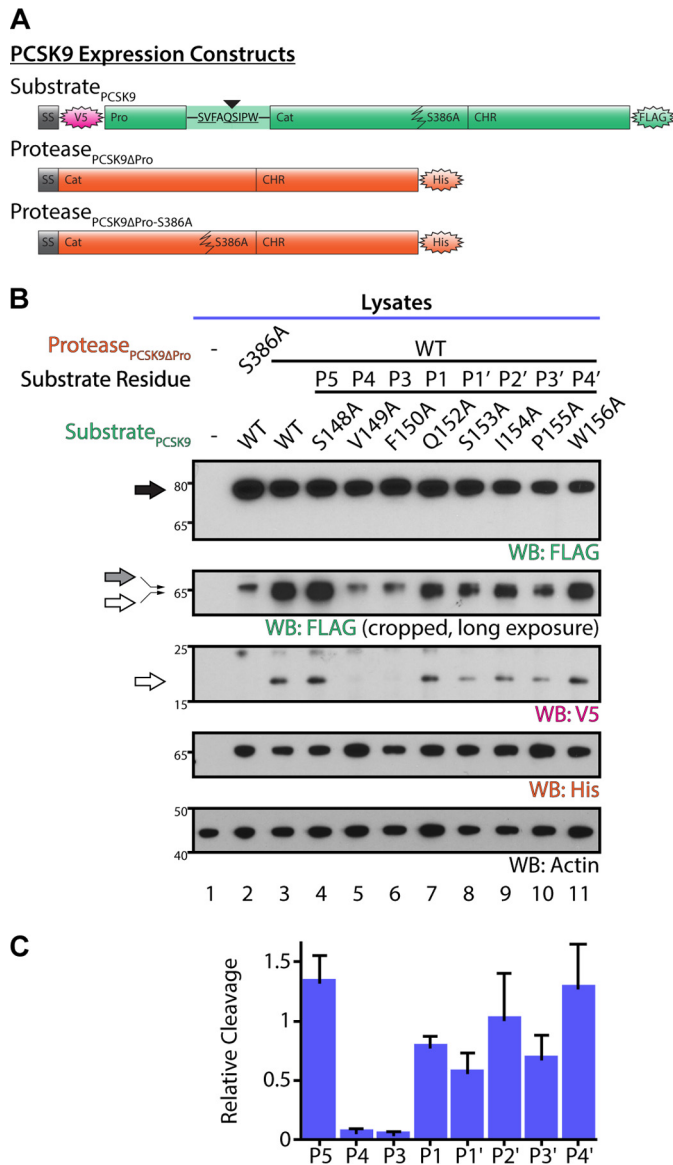**PCSK9 Expression Constructs**

B

C

FIGURE 6. **An alanine scan of the substrate cleavage sequence reveals that Val-149 and Phe-150 are critical for proteolysis.** *A*, schematics of the expression constructs are shown. The P5 through P4′ cleavage site residues spanning the prodomain/catalytic domain interface of substrate$_{PCSK9}$ are illustrated, with those targeted for alanine mutation *underlined*. *B*, Western blots (*WB*) of cell lysates of co-transfections of protease and substrate constructs as indicated. Uncleaved product is noted by the *black arrow*. Products of specific cleavage by protease$_{PCSK9\Delta Pro}$ are noted by the *open arrow*. A nonspecific cleavage product of substrate$_{PCSK9}$ is noted by the *gray arrow*. Cotransfection of unmodified substrate$_{PCSK9}$ with protease$_{PCSK9\Delta Pro}$ serves as the positive control (*lane 3*). *C*, relative cleavage of substrate$_{PCSK9}$ alanine scan mutants normalized to wild-type substrate$_{PCSK9}$ from two orthogonal readouts from two independent experiments. *Error bars* represent S.E.

protease$_{PCSK9\Delta Pro}$ and prodomain$_{Q152X}$. As expected, the wild-type residue permitted both intra- and intermolecular proteolysis (Fig. 8B, *lane 2*) as well as secretion when expressed in *trans* (Fig. 8C, *lane 2*). The clinically relevant Q152H mutation permitted some proteolysis in both systems, albeit markedly less efficiently than the wild-type (Fig. 8, *B, lane 3*, and *D, light* and *dark blue*), and was also markedly limited in secretion (Fig. 8, *C, lane 3*, and *D, purple*). The block on secretion, however, was not absolute, as secretion of Q152H (as well as for Q152I) was mildly improved when the mutant prodomain was co-ex-
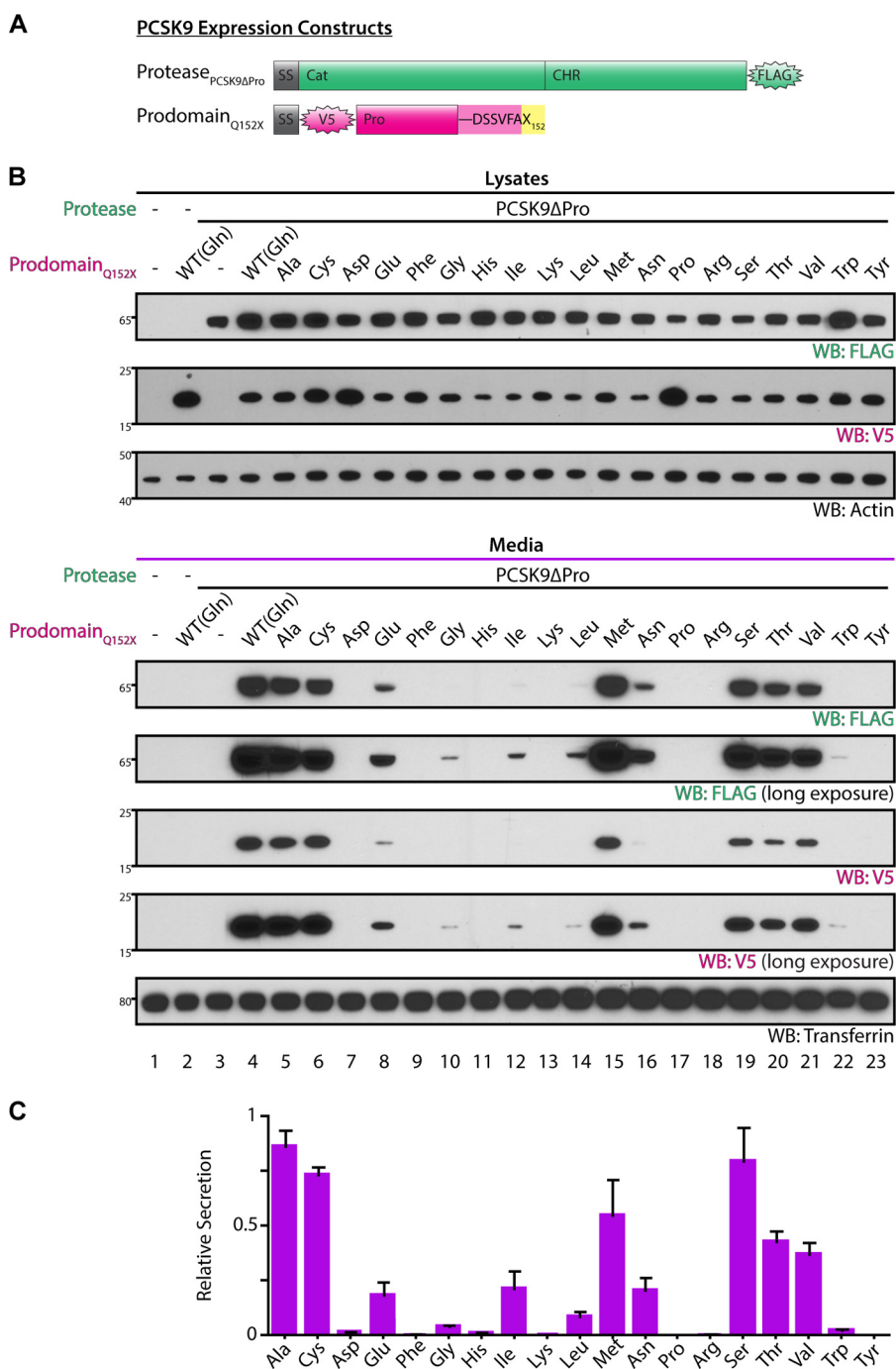
FIGURE 7. **Vertical mutagenesis strategy showing the importance of residue 152 in mediating secretion.** *A*, schematics of the expression constructs are shown. The C-terminal residues of the prodomain are illustrated for clarity, highlighted by the Q152X mutation in *yellow*, with the identity of the individual Q152X mutations noted in the subsequent blots. *B*, Western blots (*WB*) of cell lysates (*top*) and conditioned media (*bottom*) of co-transfections with the indicated protease and prodomain constructs. Co-transfection of protease$_{PCSK9\Delta Pro}$ with the wild-type prodomain serves as the positive control (*lane 4*). *C*, relative secretion of the protease$_{PCSK9\Delta Pro}$-prodomain complex for Q152X mutant, normalized to wild-type in *trans* PCSK9. Data are from two orthogonal readouts from two independent experiments, and *error bars* represent S.E.

pressed with the inactive protease$_{PCSK9\Delta Pro-S386A}$ as compared with the active protease$_{PCSK9\Delta Pro}$ (Fig. 8*C*, compare *lanes 3* and *4* with *lanes 7* and *8*). The Q152I mutation completely abrogated proteolysis in both intra- and intermolecular systems (Fig. 8, *B*, *lane 4*, and *D*) but had only a limited impact on secretion (Fig. 8, *C*, *lane 4*, and *D*, *purple*). The Q152R mutation completely abolished both proteolysis and secretion (Fig. 8, *B* and *C*, *lanes 5*, and *D*). The phenotypes of these mutations

are summarized by the schematic in Fig. 8*E*. Although each of the mutations was less permissive for either proteolysis or secretion as compared with the wild type, the illustrative finding is that certain mutations have differential effects on these two processes. These findings lend further support to our conclusion that proteolysis and secretion proceed in two independent steps mediated by different structural requirements.
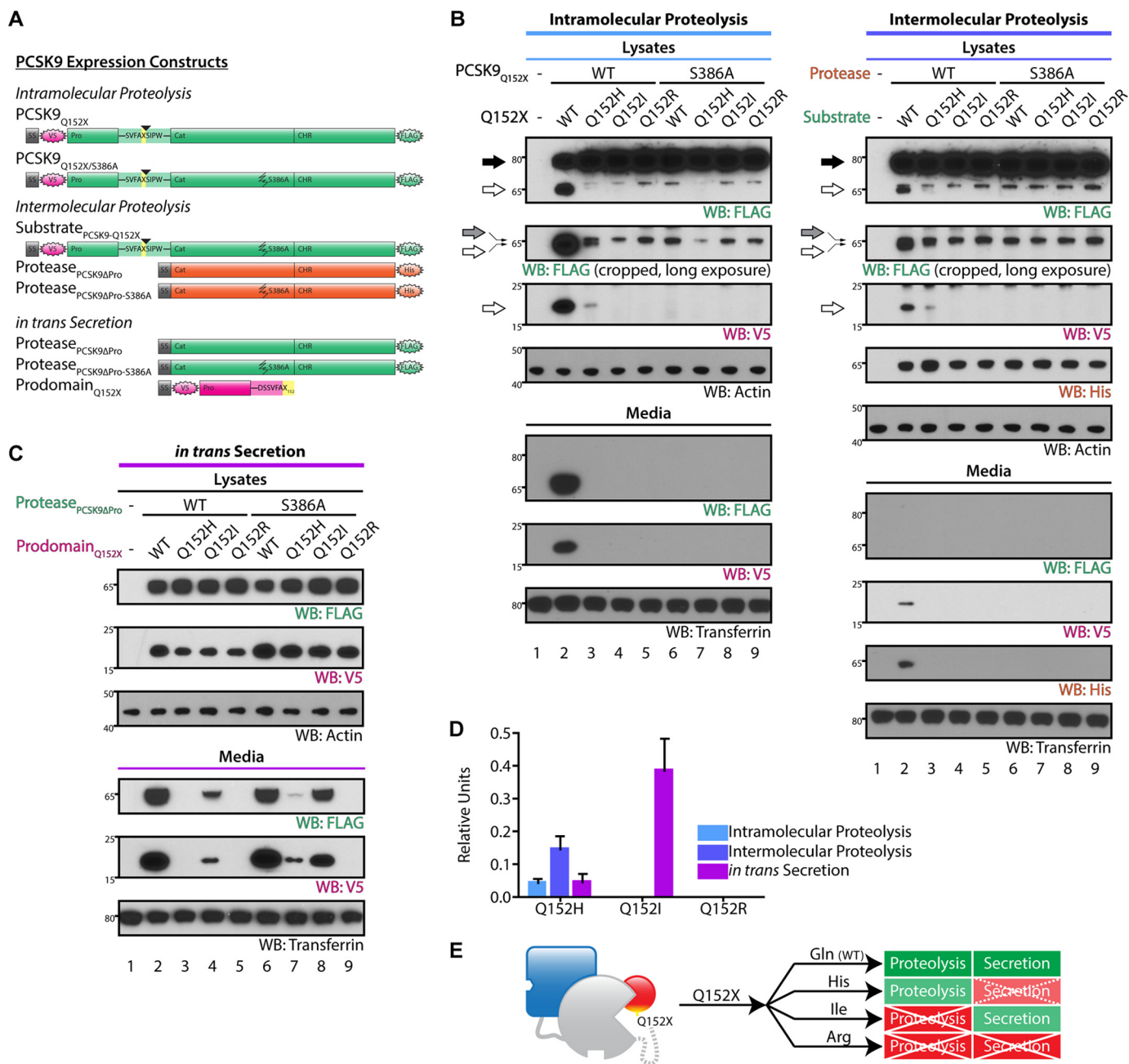
FIGURE 8. **The four phenotypes of Q152X mutants.** *A*, schematics of the expression constructs are shown grouped by experiments. Note that the protease constructs with His tags (*orange*) correspond to intermolecular proteolysis experiments, and those with FLAG tags (*green*) correspond to in *trans* secretion experiments. The Q152X mutations in the PCSK9, substrate_{PCSK9}, and prodomain constructs are highlighted in *yellow*. *B*, Western blots (*WB*) of cell lysates (*top*) and conditioned media (*bottom*) from co-transfections with PCSK9 constructs (intramolecular proteolysis, *left*) and protease and substrate constructs (intermolecular proteolysis, *right*). Uncleaved product is noted by the *black arrow*, nonspecific cleavage product by the *gray arrow*, and N- and C-terminal cleavage products noted by the *open arrows*, respectively. The wild-type Gln-152 serves as the positive control in all experiments (*lane 2*). *C*, Western blots of cell lysates (*top*) and conditioned media (*bottom*) from co-transfections with PCSK9 constructs of protease and prodomain constructs (in *trans* secretion). *D*, relative levels of intramolecular proteolysis (*light blue*), intermolecular proteolysis (*dark blue*), or in *trans* secretion (*purple*) of the Q152X mutants in the corresponding experimental system, normalized to the wild-type Gln-152. Data are from three independent experiments, and *error bars* represent S.E. *E*, schematic illustrating the phenotypes of the Q152X mutants with regard to permission of proteolysis (either intra- or intermolecular) or isolated effect on secretion (in the in *trans* system, with proteolysis bypassed). The wild-type glutamine permits both proteolysis and secretion, the histidine mutant permits some proteolysis but mainly precludes secretion, the isoleucine mutant precludes proteolysis but permits secretion, and the arginine mutant precludes both proteolysis and secretion.

DISCUSSION

In this study we began with a desire to learn more about the chemistry of the PCSK9 active site in an attempt to gain a foothold onto a highly validated therapeutic target considered too challenging to drug by binding a small molecule into the active site. We found that the PCSK9 catalytic domain has the capac-

ity to perform intermolecular proteolysis on a highly specific substrate, an orthogonally tagged but catalytically inactive proPCSK9 molecule. Furthermore, we found that such cleavage with our protease_{PCSK9ΔPro} construct was more efficient when compared with the cleavage performed by wild-type PCSK9, allowing our assay to effectively amplify the readout of intermo-

lecular PCSK9 proteolysis. We suspect that further development of this assay may be particularly useful in future screening strategies aimed at identifying small molecules or genetic targets that inhibit PCSK9 proteolysis as an ultimate means of inhibiting PCSK9's hypercholesterolemic effect. In particular, because this assay focuses on intermolecular proteolysis, it would increase the sensitivity for an initial weak inhibitor that might not be capable of out-competing an intramolecular event.

To our knowledge we present the first biochemical data that the prodomain itself acts as an inhibitor of proteolysis in *trans*. This is not surprising given that the PCSK9 structure suggests that the prodomain sterically inhibits access to the active site. The marked decrease in inhibition of intermolecular cleavage by a prodomain with a single C-terminal deletion (ΔQ152) further supports the steric hypothesis. However, additional truncations neither make the prodomain a less effective inhibitor nor disrupt binding to the catalytic domain, and as such it is tempting to speculate that another mechanism for this inhibition may be at play. We acknowledge that we have not conclusively addressed other possible mechanisms by which the truncated prodomain may affect the catalytic domain, including interference with proper folding, the formation of non-functional protein aggregates, or the binding of a motif other than the C-terminal tail that might compete against the intact prodomain of the substrate$_{PCSK9}$. Exogenous prodomain, in the form of a soluble chimeric prodomain-F_c(IgG1) fusion, has been shown to bind to mature PCSK9 independent of the CHR domain and disrupt the interaction with the LDL-R (38). Such an effect may be similar to what we are seeing here, although this remains speculation. As we ultimately chose to pursue the relationship of the prodomain to protein secretion, further evaluation of these mechanisms was outside the scope of this study.

Intriguingly, in our substrate alanine scan we found evidence of a disconnect between our intermolecular cleavage system and intramolecular proteolysis. Notably, our P3 mutant (F150A) does not undergo proteolysis, but our P3' mutant (P155A) does, which is essentially the reverse of what has previously been described for intramolecular proteolysis (16). We speculate that this disconnect relates to the method of presentation of the substrate$_{PCSK9}$ to the active site of the protease. The turn induced by Pro-155 may be required to internally align the cleavage sequence with the substrate binding groove yet may be less important for an intermolecular presentation. Likewise, the π-π stacking interaction of Phe-150 with Trp-72 may be required to drive the initial recognition of the substrate$_{PCSK9}$ with protease$_{PCSK9\Delta Pro}$ but may be less important for an intramolecular process, which has a higher effective molarity to drive the hydrolysis.

Nevertheless, the development of our intermolecular proteolysis assay allowed us to probe the impact of specific point mutations on substrate cleavage while comparing the effects of these same mutations on protein secretion in an in *trans* assay that effectively bypassed the need for proteolysis. In this manner we specifically isolated the effects of each mutation on proteolysis and secretion and found that in certain cases the results were discordant. We specifically evaluated the effect of muta-

tions at Gln-152 because the histidine mutation at this residue has been found in a hypocholesterolemic clinical cohort (36). Biochemical characterization of Q152H has previously shown that this mutant hinders PCSK9 processing by causing decreased intramolecular cleavage, leading to an intracellular accumulation of unprocessed proPCSK9 that interferes with wild-type proPCSK9 processing, producing a dominant-negative effect (37). Our results confirm the findings of the previous work; the Q152H indeed hinders intramolecular processing, and in addition, those proPCSK9$_{Q152H}$ species that manage to undergo cleavage are then subjected to an additional selection against secretion. Whether it is the proPCSK9$_{Q152H}$ or the cleaved PCSK9$_{Q152H}$ that is predominantly responsible for the dominant-negative effect remains outside the scope of this investigation but is certainly of interest.

Within the past two years two specific mediators of PCSK9 secretion have been identified: Sec24a (39) and sortilin (40). These findings lend support to the concept that PCSK9 secretion occurs in a highly regulated manner. A recent report has also suggested that the ectodomain of the LDL-R acts as a chaperone for PCSK9 folding and cleavage, increasing throughput from the proPCSK9 form to the cleaved mature form (41). Furthermore, mutations in the CHR domain, which do not affect self-proteolysis, have been noted to cause PCSK9 loss-of-function by interfering with the secretion pathway (42). Our findings build on this concept, showing that the active site and its adjacent residues can modulate both proteolysis and secretion independently. Indeed, the active site Ser-386 itself is a prime example; we suspect that the general improvement in the in *trans* secretion of prodomain mutants with the inactive protease$_{PCSK9\Delta Pro-S386A}$, as compared with active protease$_{PCSK9\Delta Pro}$, is related to improved folding of the S386A catalytic domain and subsequently improved prodomain affinity. In support of this hypothesis, we have noticed similar improvements in the yield of a heterologous bacterial expression system, which is not dependent on secretion, with the S386A mutant (data not shown). Whether the residues of the prodomain C-terminal tail are critical for mediating the interactions with Sec24a, sortilin, or the ectodomain of the LDL-R would be an informative next line of inquiry. Our mutants may also help to identify the components of the complexes, such as the putative "cargo receptor" for Sec24a, that mediate these specific secretory events. In so doing we may uncover additional targets for anti-hypercholesterolemic therapies.

The structural information we infer from these mutagenesis experiments may aid in the development of specific secretion inhibitors. Because of the proximity of our mutations to the active site as well as their marked effect on protein secretion, it is reasonable to suggest that a small molecule bound to the active site could serve as an allosteric modulator of the secretion apparatus. Although V149A mutations are expected to abolish a critical isopropyl group that projects into the PCSK9 substrate binding groove, the F150A mutation abolishes a π-π stacking interaction with Trp-72, which appears to be critical for intermolecular proteolysis but tolerated by the secretion machinery. Likewise, the proteolytic machinery appears to be at least somewhat tolerant of the histidine imidazole at position

152, whereas the secretory machinery is more tolerant of the isoleucine *sec*-butyl chain than a charged imidazole. Such differences may allow us to infer different structure-activity relationships upon scaffolds identified as either proteolysis or secretion inhibitors and help to tailor the chemistry of such scaffolds toward inhibiting one pathway *versus* another. Additionally, our data showing that the C-terminal alanine insertion after Gln-152 retained secretory activity in the in *trans* system regardless of proteolysis (Fig. 4, *D, right, lane 10*, compared with *E, lane 10*) is consistent with prior data showing that a V5 tag inserted after the prodomain C terminus acts similarly in this same system (29). Although we have not tested this C-terminal alanine insertion in either intramolecular or intermolecular proteolysis, these data do raise the question of whether additional mutations in the full-length PCSK9 protein could permit secretion despite precluding proteolysis, allowing for secretion of the proPCSK9 form. Such a mutant might allow for structural data to target the proPCSK9 species directly.

Although our initial goal was to search for a chemically feasible way to inhibit PCSK9 proteolysis, we have uncovered an additional therapeutic target that appears as promising as proteolytic inhibition. Our data suggesting the decoupling of secretion from proteolysis implies that there are two different intracellular stages at which to target PCSK9. Furthermore, an approach to specifically target secretion would theoretically have the same effect as targeting proteolysis; it would prevent PCSK9 from properly reaching the cell surface and interacting with the LDL-R. Although an intracellular mechanism of LDL-R degradation has been noted (43), it is clear from both parabiosis experiments (10) as well as the marked success of anti-PCSK9 antibodies in clinical trials (12, 13) that focusing on extracellular PCSK9 is a viable strategy. Because our data as well as that of others (37) suggest that inhibition of Q152H processing is in part mediated by a specific block on secretion, such a strategy would inch even closer to phenocopying this known genetic mutation. Given that this mutation is both dominant negative and is well tolerated (indeed, cardioprotective) in individuals, we see this as further encouragement for such an approach.

REFERENCES

1. Park, S. W., Moon, Y.-A., and Horton, J. D. (2004) Post-transcriptional regulation of low density lipoprotein receptor protein by proprotein convertase subtilisin/kexin type 9a in mouse liver. *J. Biol. Chem.* **279,** 50630–50638
2. Maxwell, K. N., and Breslow, J. L. (2004) Adenoviral-mediated expression of Pcsk9 in mice results in a low-density lipoprotein receptor knockout phenotype. *Proc. Natl. Acad. Sci. U.S.A.* **101,** 7100–7105
3. Abifadel, M., Varret, M., Rabès, J.-P., Allard, D., Ouguerram, K., Devillers, M., Cruaud, C., Benjannet, S., Wickham, L., Erlich, D., Derré, A., Villéger, L., Farnier, M., Beucler, I., Bruckert, E., Chambaz, J., Chanu, B., Lecerf, J.-M., Luc, G., Moulin, P., Weissenbach, J., Prat, A., Krempf, M., Junien, C., Seidah, N. G., and Boileau, C. (2003) Mutations in PCSK9 cause autosomal dominant hypercholesterolemia. *Nat. Genet.* **34,** 154–156
4. Cohen, J., Pertsemlidis, A., Kotowski, I. K., Graham, R., Garcia, C. K., and Hobbs, H. H. (2005) Low LDL cholesterol in individuals of African descent resulting from frequent nonsense mutations in PCSK9. *Nat. Genet.* **37,** 161–165
5. Cohen, J. C., Boerwinkle, E., Mosley, T. H., Jr., and Hobbs, H. H. (2006) Sequence variations in PCSK9, low LDL, and protection against coronary heart disease. *N. Engl. J. Med.* **354,** 1264–1272
6. Tosi, I., Toledo-Leiva, P., Neuwirth, C., Naoumova, R. P., and Soutar, A. K. (2007) Genetic defects causing familial hypercholesterolaemia: identification of deletions and duplications in the LDL-receptor gene and summary of all mutations found in patients attending the Hammersmith Hospital Lipid Clinic. *Atherosclerosis* **194,** 102–111
7. Zhao, Z., Tuakli-Wosornu, Y., Lagace, T. A., Kinch, L., Grishin, N. V., Horton, J. D., Cohen, J. C., and Hobbs, H. H. (2006) Molecular characterization of loss-of-function mutations in PCSK9 and identification of a compound heterozygote. *Am. J. Hum. Genet.* **79,** 514–523
8. Poirier, S., Mayer, G., Benjannet, S., Bergeron, E., Marcinkiewicz, J., Nassoury, N., Mayer, H., Nimpf, J., Prat, A., and Seidah, N. G. (2008) The proprotein convertase PCSK9 induces the degradation of low density lipoprotein receptor (LDLR) and its closest family members VLDLR and ApoER2. *J. Biol. Chem.* **283,** 2363–2372
9. McNutt, M. C., Kwon, H. J., Chen, C., Chen, J. R., Horton, J. D., and Lagace, T. A. (2009) Antagonism of secreted PCSK9 increases low density lipoprotein receptor expression in HepG2 cells. *J. Biol. Chem.* **284,** 10561–10570
10. Lagace, T. A., Curtis, D. E., Garuti, R., McNutt, M. C., Park, S. W., Prather, H. B., Anderson, N. N., Ho, Y. K., Hammer, R. E., and Horton, J. D. (2006) Secreted PCSK9 decreases the number of LDL receptors in hepatocytes and in livers of parabiotic mice. *J. Clin. Invest.* **116,** 2995–3005
11. Kwon, H. J., Lagace, T. A., McNutt, M. C., Horton, J. D., and Deisenhofer, J. (2008) Molecular basis for LDL receptor recognition by PCSK9. *Proc. Natl. Acad. Sci. U.S.A.* **105,** 1820–1825
12. Stein, E. A., Mellis, S., Yancopoulos, G. D., Stahl, N., Logan, D., Smith, W. B., Lisbon, E., Gutierrez, M., Webb, C., Wu, R., Du, Y., Kranz, T., Gasparino, E., and Swergold, G. D. (2012) Effect of a monoclonal antibody to PCSK9 on LDL cholesterol. *N. Engl. J. Med.* **366,** 1108–1118
13. Blom, D. J., Hala, T., Bolognese, M., Lillestol, M. J., Toth, P. D., Burgess, L., Ceska, R., Roth, E., Koren, M. J., Ballantyne, C. M., Monsalvo, M. L., Tsirtsonis, K., Kim, J. B., Scott, R., Wasserman, S. M, Stein, E. A., DESCARTES Investigators. (2014) A 52-week placebo-controlled trial of evolocumab in hyperlipidemia. *N. Engl. J. Med.* **370,** 1809–1819
14. Fitzgerald, K., Frank-Kamenetsky, M., Shulga-Morskaya, S., Liebow, A., Bettencourt, B. R., Sutherland, J. E., Hutabarat, R. M., Clausen, V. A., Karsten, V., Cehelsky, J., Nochur, S. V., Kotelianski, V., Horton, J., Mant, T., Chiesa, J., Ritter, J., Munisamy, M., Vaishnaw, A. K., Gollob, J. A., and Simon, A. (2014) Effect of an RNA interference drug on the synthesis of proprotein convertase subtilisin/kexin type 9 (PCSK9) and the concentration of serum LDL cholesterol in healthy volunteers: a randomised, single-blind, placebo-controlled, phase 1 trial. *Lancet.* **383,** 60–68
15. Seidah, N. G., Awan, Z., Chrétien, M., and Mbikay, M. (2014) PCSK9: a key modulator of cardiovascular health. *Circ. Res.* **114,** 1022–1036
16. Benjannet, S., Rhainds, D., Essalmani, R., Mayne, J., Wickham, L., Jin, W., Asselin, M. C., Hamelin, J., Varret, M., Allard, D., Trillard, M., Abifadel, M., Tebon, A., Attie, A. D., Rader, D. J., Boileau, C., Brissette, L., Chrétien, M., Prat, A., and Seidah, N. G. (2004) NARC-1/PCSK9 and its natural mutants: zymogen cleavage and effects on the low density lipoprotein (LDL) receptor and LDL cholesterol. *J. Biol. Chem.* **279,** 48865–48875
17. Naureckiene, S., Ma, L., Sreekumar, K., Purandare, U., Lo, C. F., Huang, Y., Chiang, L. W., Grenier, J. M., Ozenberger, B. A., Jacobsen, J. S., Kennedy, J. D., DiStefano, P. S., Wood, A., and Bingham, B. (2003) Functional characterization of Narc 1, a novel proteinase related to proteinase K. *Arch. Biochem. Biophys.* **420,** 55–67
18. Seidah, N. G., Benjannet, S., Wickham, L., Marcinkiewicz, J., Jasmin, S. B., Stifani, S., Basak, A., Prat, A., and Chretien, M. (2003) The secretory proprotein convertase neural apoptosis-regulated convertase 1 (NARC-1): liver regeneration and neuronal differentiation. *Proc. Natl. Acad. Sci.*

U.S.A. **100,** 928–933

19. Nassoury, N., Blasiole, D. A., Tebon Oler, A., Benjannet, S., Hamelin, J., Poupon, V., McPherson, P. S., Attie, A. D., Prat, A., and Seidah, N. G. (2007) The cellular trafficking of the secretory proprotein convertase PCSK9 and its dependence on the LDLR. *Traffic* **8,** 718–732

20. Maxwell, K. N., Fisher, E. A., and Breslow, J. L. (2005) Overexpression of PCSK9 accelerates the degradation of the LDLR in a post-endoplasmic reticulum compartment. *Proc. Natl. Acad. Sci. U.S.A.* **102,** 2069–2074

21. Seidah, N. G., and Prat, A. (2012) The biology and therapeutic targeting of the proprotein convertases. *Nat. Rev. Drug Discov.* **11,** 367–383

22. Cunningham, D., Danley, D. E., Geoghegan, K. F., Griffor, M. C., Hawkins, J. L., Subashi, T. A., Varghese, A. H., Ammirati, M. J., Culp, J. S., Hoth, L. R., Mansour, M. N., McGrath, K. M., Seddon, A. P., Shenolikar, S., Stutzman-Engwall, K. J., Warren, L. C., Xia, D., and Qiu, X. (2007) Structural and biophysical studies of PCSK9 and its mutants linked to familial hypercholesterolemia. *Nat. Struct. Mol. Biol.* **14,** 413–419

23. Kourimate, S., Chétiveaux, M., Jarnoux, A. L., Lalanne, F., and Costet, P. (2009) Cellular and secreted pro-protein convertase subtilisin/kexin type 9 catalytic activity in hepatocytes. *Atherosclerosis* **206,** 134–140

24. Piper, D. E., Jackson, S., Liu, Q., Romanow, W. G., Shetterly, S., Thibault, S. T., Shan, B., and Walker, N. P. (2007) The crystal structure of PCSK9: a regulator of plasma LDL-cholesterol. *Structure* **15,** 545–552

25. Rahuel, J., Rasetti, V., Maibaum, J., Rüeger, H., Göschke, R., Cohen, N. C., Stutz, S., Cumin, F., Fuhrer, W., Wood, J. M., and Grütter, M. G. (2000) Structure-based drug design: the discovery of novel nonpeptide orally active inhibitors of human renin. *Chem. Biol.* **7,** 493–504

26. Maibaum, J., Stutz, S., Göschke, R., Rigollier, P., Yamaguchi, Y., Cumin, F., Rahuel, J., Baum, H. P., Cohen, N. C., Schnell, C. R., Fuhrer, W., Gruetter, M. G., Schilling, W., and Wood, J. M. (2007) Structural modification of the P2′ position of 2,7-dialkyl-substituted 5(*S*)-amino-4(*S*)-hydroxy-8-phenyl-octanecarboxamides: the discovery of aliskiren, a potent nonpeptide human renin inhibitor active after once daily dosing in marmosets. *J. Med. Chem.* **50,** 4832–4844

27. Liu, H., and Naismith, J. H. (2008) An efficient one-step site-directed deletion, insertion, single and multiple-site plasmid mutagenesis protocol. *BMC Biotechnol.* **8,** 91

28. Gibson, D. G., Young, L., Chuang, R.-Y., Venter, J. C., Hutchison, C. A., 3rd, and Smith, H. O. (2009) Enzymatic assembly of DNA molecules up to several hundred kilobases. *Nat. Methods* **6,** 343–345

29. McNutt, M. C., Lagace, T. A., and Horton, J. D. (2007) Catalytic activity is not required for secreted PCSK9 to reduce low density lipoprotein receptors in HepG2 cells. *J. Biol. Chem.* **282,** 20799–20803

30. Du, F., Hui, Y., Zhang, M., Linton, M. F., Fazio, S., and Fan, D. (2011) Novel domain interaction regulates secretion of proprotein convertase subtilisin/kexin type 9 (PCSK9) protein. *J. Biol. Chem.* **286,** 43054–43061

31. Hampton, E. N., Knuth, M. W., Li, J., Harris, J. L., Lesley, S. A., and Spraggon, G. (2007) The self-inhibited structure of full-length PCSK9 at 1.9 Å reveals structural homology with resistin within the C-terminal domain. *Proc. Natl. Acad. Sci. U.S.A.* **104,** 14604–14609

32. Seidah, N. G., Sadr, M. S., Chrétien, M., and Mbikay, M. (2013) The multifaceted proprotein convertases: their unique, redundant, complementary, and opposite functions. *J. Biol. Chem.* **288,** 21473–21481

33. Fu, X., Inouye, M., Shinde, U. (2000) Folding pathway mediated by an intramolecular chaperone. The inhibitory and chaperone functions of the subtilisin propeptide are not obligatorily linked. *J. Biol. Chem.* **275,** 16871–16878

34. Anderson, E. D., VanSlyke, J. K., Thulin, C. D., Jean, F., and Thomas, G. (1997) Activation of the furin endoprotease is a multiple-step process: requirements for acidification and internal propeptide cleavage. *EMBO J.* **16,** 1508–1518

35. Nguyen, A. W., and Daugherty, P. S. (2005) Evolutionary optimization of fluorescent proteins for intracellular FRET. *Nat. Biotechnol.* **23,** 355–360

36. Mayne, J., Dewpura, T., Raymond, A., Bernier, L., Cousins, M., Ooi, T. C., Davignon, J., Seidah, N. G., Mbikay, M., and Chrétien, M. (2011) Novel loss-of-function PCSK9 variant is associated with low plasma LDL cholesterol in a French-Canadian family and with impaired processing and secretion in cell culture. *Clin. Chem.* **57,** 1415–1423

37. Benjannet, S., Hamelin, J., Chrétien, M., and Seidah, N. G. (2012) Loss- and gain-of-function PCSK9 variants: cleavage specificity, dominant negative effects, and low density lipoprotein receptor (LDLR) degradation. *J. Biol. Chem.* **287,** 33745–33755

38. Saavedra, Y. G., Zhang, J., and Seidah, N. G. (2013) PCSK9 prosegment chimera as novel inhibitors of LDLR degradation. *PLoS ONE* **8,** e72113

39. Chen, X.-W., Wang, H., Bajaj, K., Zhang, P., Meng, Z. X., Ma, D., Bai, Y., Liu, H. H., Adams, E., Baines, A., Yu, G., Sartor, M. A., Zhang, B., Yi, Z., Lin, J., Young, S. G., Schekman, R., and Ginsburg, D. (2013) SEC24A deficiency lowers plasma cholesterol through reduced PCSK9 secretion. *Elife* **2,** e00444

40. Gustafsen, C., Kjolby, M., Nyegaard, M., Mattheisen, M., Lundhede, J., Buttenschøn, H., Mors, O., Bentzon, J. F., Madsen, P., Nykjaer, A., and Glerup, S. (2014) The hypercholesterolemia-risk gene SORT1 facilitates PCSK9 secretion. *Cell Metab.* **19,** 310–318

41. Strøm, T. B., Tveten, K., and Leren, T. P. (2014) PCSK9 acts as a chaperone for the LDL receptor in the endoplasmic reticulum. *Biochem. J.* **457,** 99–105

42. Cameron, J., Holla, Ø. L., Laerdahl, J. K., Kulseth, M. A., Berge, K. E., and Leren, T. P. (2009) Mutation S462P in the PCSK9 gene reduces secretion of mutant PCSK9 without affecting the autocatalytic cleavage. *Atherosclerosis* **203,** 161–165

43. Poirier, S., Mayer, G., Poupon, V., McPherson, P. S., Desjardins, R., Ly, K., Asselin, M. C., Day, R., Duclos, F. J., Witmer, M., Parker, R., Prat, A., and Seidah, N. G. (2009) Dissection of the endogenous cellular pathways of PCSK9-induced low density lipoprotein receptor degradation: evidence for an intracellular route. *J. Biol. Chem.* **284,** 28856–28864